



1
2
3
4

5 **Title:** Comment on “Identification of the IMF sector structure in near-real time by ground magnetic
6 data” by Janzhura and Troshichev (2011).

7

8 **Author:** Peter Stauning, Danish Meteorological Institute, Lyngbyvej 100, Copenhagen.

9 Mail: pst@dmi.dk

10

11

12 **Abstract.** The only published description of the solar wind sector (SS) term used for the reference
13 level in the post-event and real-time derivation of the Polar Cap (PC) indices, PCN (North) and PCS
14 (South), in the version endorsed by the International Association for Geomagnetism and Aeronomy
15 (IAGA) is found in the commented publication, Janzhura and Troshichev: Identification of the IMF
16 sector structure in near-real time by ground magnetic data, Annales Geophysicae, 29, 1491-1500,
17 2011. Actually, the publication has served as basis for the index endorsement by IAGA in 2013.
18 However, neither the illustrations nor the results presented there have been derived by the specified
19 near-real time method. Figs. 1, 6, 7, and 8 display values derived by post-event calculations based
20 on daily medians smoothed over 7 days centred on the day of interest. Figs. 2, 3, and 4 display
21 observed values smoothed over 7 days, while the remaining Fig. 5 displays averages over 4 months.
22 In summary, there are strong disagreements between indications in the title, abstract, and statements
23 in the text compared to the actual results and their illustrations.

24

25

26

1. Introduction

27 The derivation of the Polar Cap (PC) indices, PCN (North) based on Qaanaaq data and PCS (South)
28 based on Vostok data, in the versions endorsed by the International Association for Geomagnetism
29 and Aeronomy (IAGA) in Resolution #3 (2013) is to a large extent based on the methods described
30 in Janzhura and Troshichev (2011): Identification of the IMF sector structure in near-real time by
31 ground magnetic data (hereinafter J&T2011) (and its replicate in Troshichev and Janzhura, 2012,
32 hereinafter T&J2012). This work provides the only published description of the solar wind sector
33 (SS) term related to the Y-component, IMF B_Y , of the interplanetary magnetic field (IMF). The SS
34 terms are derived from daily median values of the recorded magnetic field components and added to
35 the index reference level in the post-event or near-real time versions. For post-event PC index
36 calculations the SS-terms are derived from 7-days averaging of daily median values of the recorded
37 magnetic data. For the near-real time calculations the SS-terms are derived from cubic spline-based
38 forward extrapolation of past median values.

39

40

41

42

43

44

45

46

47

However, the method is invalid since it assumes that the IMF B_Y -related effects originating at the
dayside Cusp region can be compensated for by using a daily median-based SS-term at all local
hours. Instead, the addition of this singular term to the index reference level generates unfounded
positive or negative PC index contributions at different observatory positions along its daily path
with respect to the polar cap ionosphere. The solar wind sector “compensation”, typically, generates
unfounded contributions to the PC indices at the night side although the real IMF B_Y effects on
polar magnetic fields at the night side are usually very small. Correspondingly, the “compensation”
might have little effect on PC indices at the dayside although the Cusp-related IMF B_Y effects
maximize there.



48 An example case gave an unfounded change of 2.45 mV/m (magnetic storm level according to
49 Troshichev et al., 2017) at local midnight and hardly any effect at noon at 4 nT amplitude in
50 smoothed IMF B_Y values which is a common occurrence (Stauning, 2015).

51

52

53 2. Calculation of IMF B_Y -related solar wind sector term

54 The commented publication, J&T2011, holds (p.1496-97) a step-by-step procedure quoted below
55 for near-real time calculations of IMF B_Y -related solar wind sector (SS) terms by forward cubic
56 spline-based extrapolation of past median values:

57 *“Keeping in mind this specification, the 3-day smoothing averages of the median values were subjected to*
58 *the interpolation procedure including the following steps:*

59 1. *median values for magnetic components H and D are derived for 4 intervals of days preceding with the*
60 *exception of the current day (n=0):*

61 - $r1=F$ [for interval from n-3 day to n-1 day]

62 - $r2=F$ [for interval from n-5 day to n-3 day]

63 - $r3=F$ [for interval from n-7 day to n-5 day]

64 - $r4=F$ [for interval from n-9 day to n-7 day];

65 2. *piecewise polynomial form of the cubic spline interpolant for r1, r2, r3, and r4 segments is determined;*

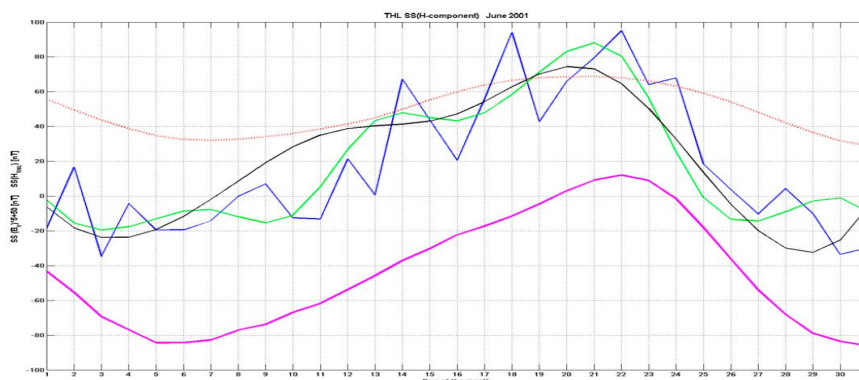
66 3. *termination of this form related to day n=0 is examined as representative of the SS effect for the current*
67 *day, even if this day is disturbed.*

68 *The procedure is repeated each subsequent day. Results of the procedure – the variation of the reconstructed magnetic*
69 *H component is presented by the magenta line in the same Fig. 6, the reconstructed H-component curve being shifted by*
70 *50 nT to a lower position”*

71 Thus, it is stated (p. 1497) that this procedure was used to derive the smoothly varying display of
72 the H-component SS-term (magenta line) in their Fig. 6 using magnetic data from Qaanaaq (THL)
73 for the interval 1-30 June 2001, here reproduced in Fig. 1 and re-calculated in Fig. 2. However, the
74 statement concluding the quoted procedure is incorrect. The SS-term (H_{SS}) displayed in Fig. 6 of
75 J&T2011 could not have been generated by the quoted near-real time procedure. The smoothed
76 magenta curve for H_{SS} is not a real-time version but derived by using the post-event method based
77 on daily median values smoothed over 7 days with the actual day at the middle. Fig. 2 presents the
78 post-event (“final”) H_{SS} values derived by the PCN index suppliers at the Danish Space Research
79 Institute (DTU Space).

80 Values of the solar wind sector term, H_{SS} , derived by adhering rigorously to the above quoted
81 “near-real time” procedure (including the cubic spline-based forward projection) are displayed by
82 the jagged curve in magenta line in Fig. 3.

83



84

Fig. 6. Behavior of the median values of the magnetic H-component at Thule station during June months of 1998 (a) and 2001 (b) for intervals with duration of 1 day (blue line), 3 days (green line), and 5 days (black line). The red dotted line shows the variation of the IMF B_y component, derived from spacecraft measurements. The magenta line shows the variation of the reconstructed magnetic H-component. To be clearly demonstrated, the actual B_y values were multiplied by five and were shifted by 50 nT to a higher position, whereas the curve of reconstructed H-component was shifted by 50 nT to a lower position.

85

86

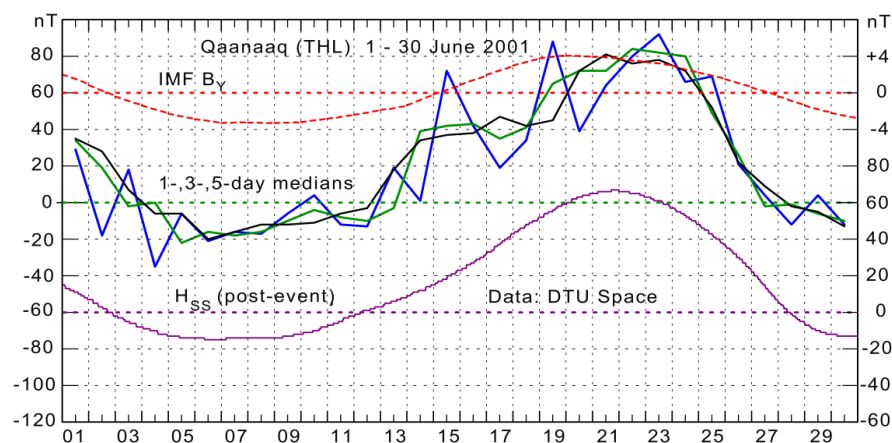
87

Fig. 1. THL H-component. 1-day (blue line), 3-days (green) and 5-days (black) median values. Resulting H_{SS} terms in magenta line on a scale shifted 50 nT downward for clarity. Smoothed IMF B_y multiplied by 5 and shifted 50 nT upward in red line. (Reproduced from Fig. 6b of Janzhura and Troshichev, 2011, including caption).

89

90

91



92

93

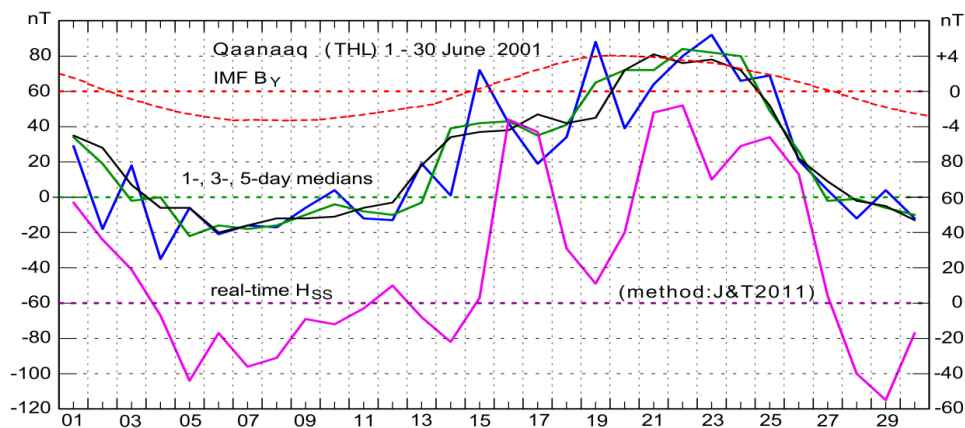
94

Fig. 2. THL 1-, 3-, 5-day medians on left scale. Post-event H_{SS} terms are displayed in magenta line on lower right scale. The data were supplied from DTU Space. Smoothed IMF B_y values (red line) added on upper right scale (data from OMNIweb).

95

96

97



98
 99

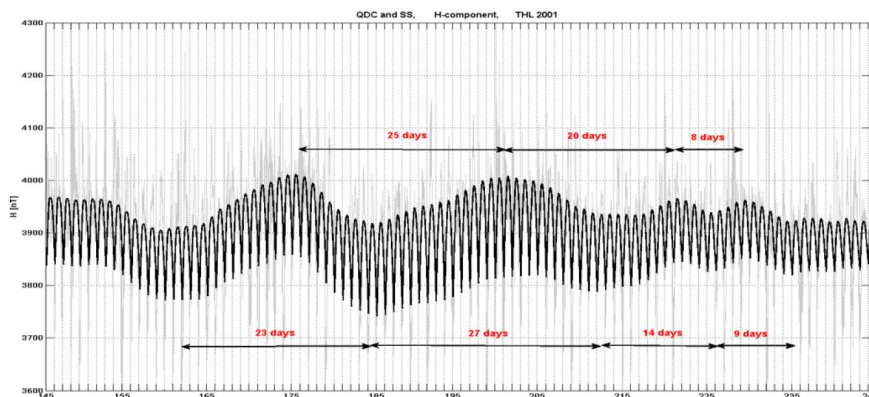
100 **Fig. 3.** THL 1-, 3-, 5-day medians on left scale. Simulated real-time H_{SS} terms in magenta line on lower
 101 right scale. H_{SS} values were calculated by following exactly the procedure in J&T2011.(Stauning, 2018a).
 102 Smoothed IMF B_Y values added on upper right scale (OMNIweb)
 103

104 The similarity between the H_{SS} curves in Figs.1 and 2 and the large difference with respect to the
 105 simulated real-time H_{SS} values in Fig.3 derived from cubic spline-based extrapolation of past
 106 median values implies that the display in Fig. 6 of J&T2011 (Fig. 4.15 of T&J2012), contrary to the
 107 statement in p. 1496-97, was actually generated by using post-event calculations with smoothed
 108 averages of 7 days daily median values.

109

110 3. Use of Solar Wind Sector (SS) term in reference level for PC indices.

111 The IMF B_Y -related solar wind sector effects on the convection patterns generate changes in the PC
 112 index response to the merging electric fields. The solar wind sector (SS) term was implemented in
 113 the derivation of PC index reference levels by J&T2011. The SS-term from their Fig. 6 has been
 114 added to the quiet day variation (QDC) with slowly (seasonally) varying amplitude calculated by
 115 the method published in Janzhura and Troshichev (2008) to generate the June section (days 152-
 116 182) of the reference level displayed by the solid line superimposed on the 1-min H-component
 117 values displayed in their Fig.1. The remaining part of the reference levels has no doubt been
 118 generated by the same method reproduced here in Fig. 4 (including caption) and recalculated in Fig.
 119 5. However, using the near-real time H_{SS} version generates the jagged reference level displayed in
 120 red solid line superimposed on the H-component values displayed in faint blue line in Fig. 6.
 121



122

Fig. 1. Superposition of the actual variation of 1-min values of the geomagnetic H-component observed at Thule station in the summer season of 2001 (thin lines) and the quiet daily curve (QDC) characterizing the daily variation of the quiet geomagnetic field (thick solid lines).

123

124

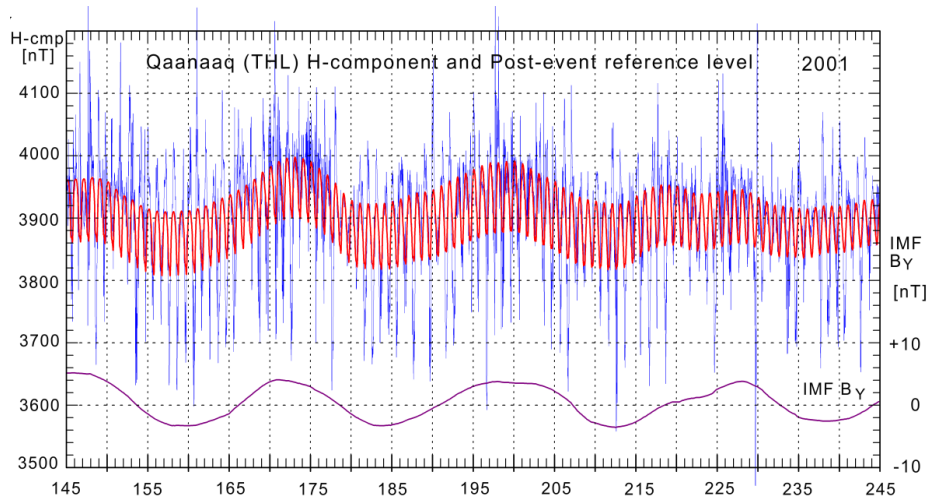
125

126

127

128

Fig. 4. PCN reference level (thick line) superimposed on recorded H-component data (thin line).
Reproduction of Fig. 1 of Janzhura and Troshichev (2011), (caption included).



129

130

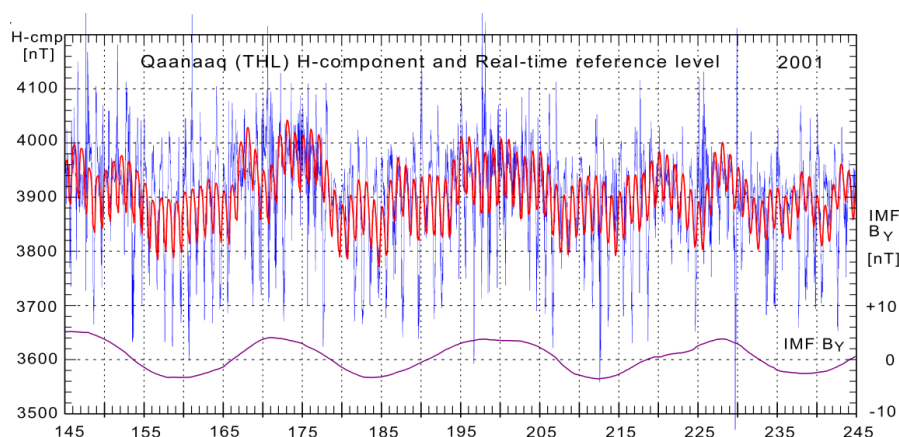
131

132

133

134

Fig. 5. Post-event (final) PCN reference level values (red line) supplied from DTU Space superimposed on recorded H-component data (blue line). IMF B_y values (magenta line) on the lower right scale added at the bottom of the diagram for reference. (after Stauning, 2015).



135
136
137
138
139
140

Fig. 6. Simulated real-time PCN reference level (red line) derived by rigorous use of the J&T2011 procedure superimposed on recorded H-component data (blue line). IMF B_Y values added at the bottom of the diagram.

141
142
143
144
145
146

The close similarity of the reference level (thick line) in Fig. 4 with that of Fig. 5 and the strong difference with respect to the real-time reference level in Fig. 6 implies that the “QDC” in Fig. 4 was actually derived by the post-event (final) calculation method (7-days smoothing of daily median H-component values) like the method used for Fig. 5.

147
148
149
150
151
152
153
154

4. The SS-effects throughout a year (2001).

Figure 7b in J&T2011 (Fig. 4.16b in T&J2012) displays the H-component recorded at Qaanaaq (THL) throughout year 2001. The IMF B_Y -related H_{SS} values have been superimposed on the recordings. According to the description, the black asterisks present near-real time values, while the red asterisks present post-event values. It appears that the two sets of symbols merge to form a smooth continuous curve. However, contrary to the description in text and figure caption, both symbol series have been generated by post-event calculation methods (averaged daily median values).

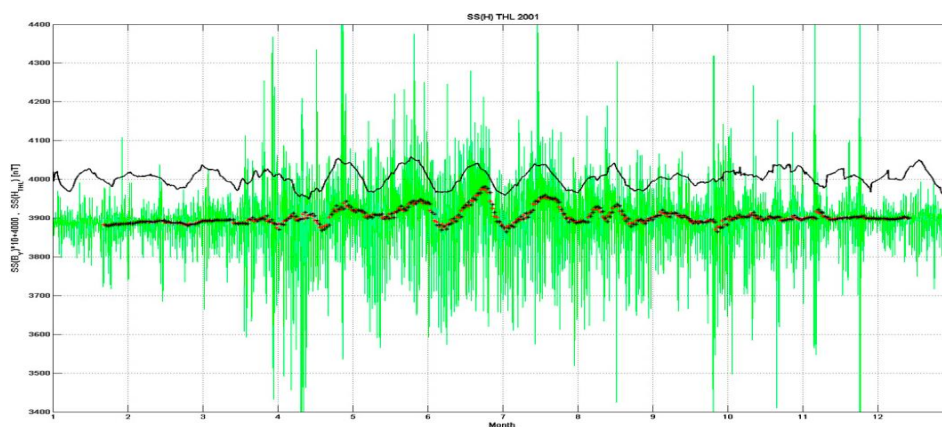
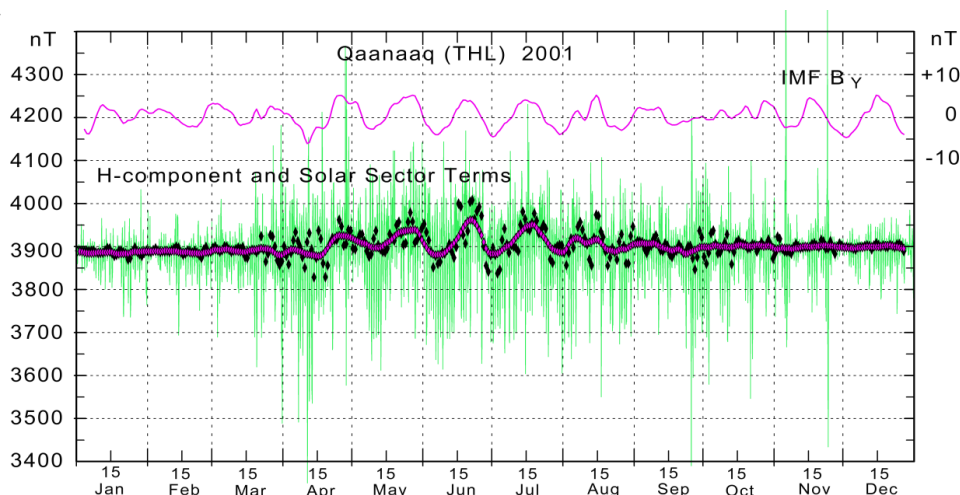


Fig. 7. The SS effect derived in the H-component observed at station Thule in 1998 (a) and 2001 (b). The actual variation of the ground H-component is shown by the green line, whereas black asterisks present the extrapolated SS structure obtained by the extrapolation procedure when all data are available till the examined day ($n = 0$), and red asterisks present the interpolated SS structure derived under the condition that the examined day is in the middle of a gap in the time interval. The actual variation of the IMF B_y component, measured by ACE spacecraft, is shown by the thin black line.

155
 156
 157
 158
 159
 160
 161
 162
 163
 164

Fig. 7. Presentation of one year's THL H-component data (green line) with superimposed near-real time (black), and post-event H_{SS} values (red asterisks). IMF B_y values added (black line). Reproduced from Fig. 7b of Janzura and Troshichev (2011) (caption included).

Re-calculated values are displayed in Fig. 8 where the post-event symbols (magenta diamonds) merge to form a continuous broad trace of H_{SS} values. The scattered near-real time symbols (black diamonds) have been calculated by using rigorously the J&T2011 near-real time procedure quoted above.



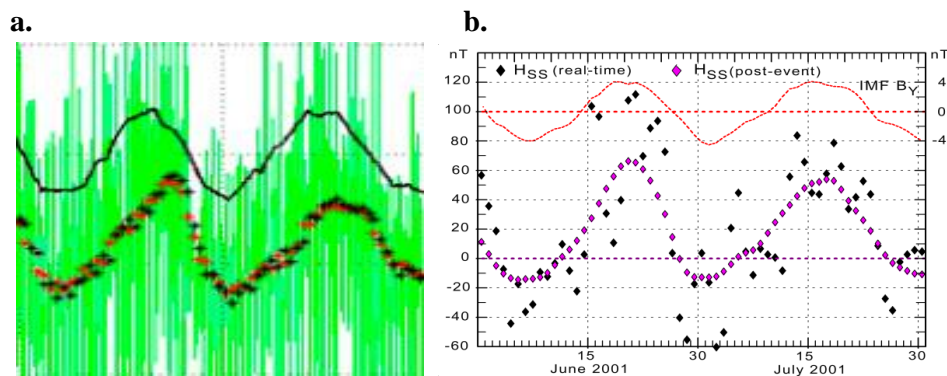
165
 166
 167
 168
 169

Fig. 8. THL H-component data with superimposed simulated real-time (black), and post-event (magenta diamonds) values of H_{SS} . Note the large scatter of the real-time (black) diamonds. IMF B_y values added (red line) on upper right scale.



170

171 Figs. 9a, b provide more detailed comparisons of the values displayed in Figs. 7 and 8.



172

173 **Fig. 9.** (a) Detailed plot of June-July section of Fig. 7 from Janzhura and Troshichev (2011). Note the almost
 174 continuous transition from black to red diamonds. IMF B_Y values added (black line). (b) Details of Fig. 8.
 175 Note the large scatter in the black diamonds (simulated real-time) away from the post-event magenta
 176 diamond symbols. IMF B_Y values added for reference (red line).

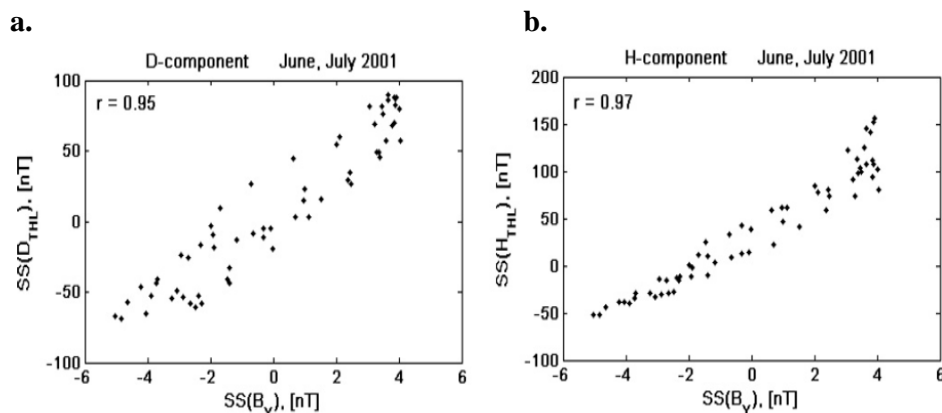
177

178 It is evident from Figs. 8 and 9b that the real-time and post-event methods generate quite different
 179 values of the IMF B_Y -related solar wind sector terms, H_{SS} . The set of red asterisks in Figs. 7 and 9a,
 180 no doubt, present post-event (smoothed daily median) values, while the black set in Figs. 7 and 9a,
 181 against the statements in the text and in the figure caption, could not present near-real time values
 182 but must have been derived by post event smoothing.

183
 184
 185

186 5. Identification of solar wind sector structure in near real time

187 Fig. 8b of J&T2011 reproduced here in Fig. 10 display close relations between solar sector terms
 188 D_{SS} and H_{SS} and daily average IMF B_Y values. These relations are assumed to enable the possible
 189 identification of the IMF sector structure in near-real time (title of the publication).



190

191 **Fig. 8.** The relationship between the satellite and ground-based sets of magnetic data on variations caused by the IMF sector structure in the
 192 summer months of 1998 (upper row) and 1991 (lower row) for geomagnetic D (left column) and H (right column) components at Thule.

192



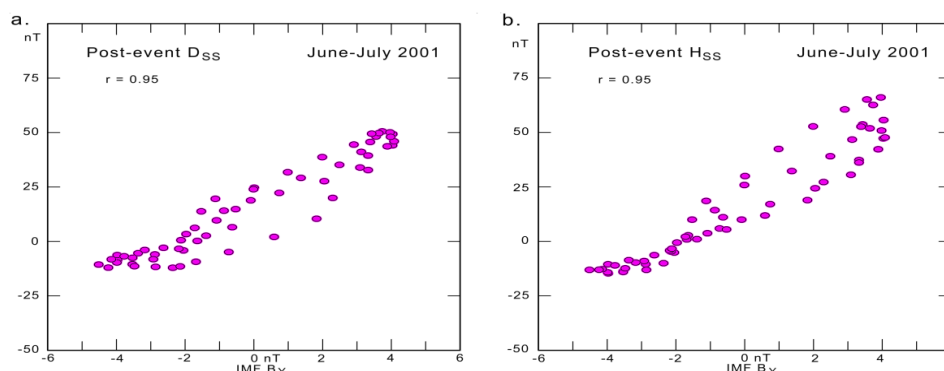
193

194 **Fig. 10.** Reproduction of Fig. 8b from Janzhura and Troshichev (2011) (incl. caption). Relations between
195 daily average IMF B_Y values and solar wind sector (a) D_{SS} and (b) H_{SS} values. Note: Scale values are by
196 some error (misprint) too large by a factor 2.

197

198 D_{SS} and H_{SS} values for the summer months, June-July, 2001, provided by DTU-Space are displayed
199 in Figs. 11a,b (left and right). The values have been calculated from the 7-days averaged daily
200 median D- and H-component values using the post-event method.

201



202

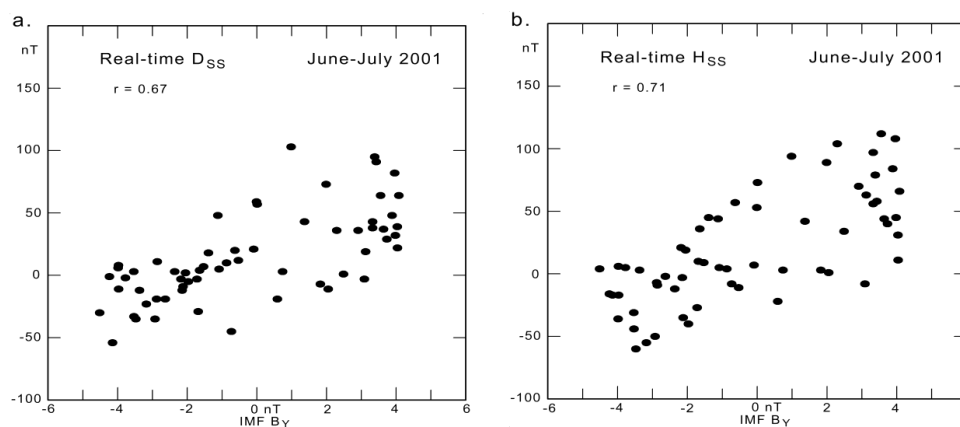
203 **Fig. 11.** Display of post-event (final) solar wind sector terms, D_{SS} , H_{SS} , supplied from DTU Space vs. daily
204 average IMF B_Y values. Note, that the scales are reduced by factor 2 from those of Fig. 10 to correct the
205 scaling errors in Fig. 8 of J&T2011.

206

207 The corresponding near-real time values of D_{SS} and H_{SS} for June-July, 2001, have been calculated
208 by rigorous use of the above quoted near-real time procedure from J&T2011. The results are
209 displayed in Figs. 12a,b.

210

211



212

213 **Fig. 12.** Display of simulated real-time solar wind sector terms, D_{SS} , H_{SS} , calculated by using the procedure
214 in J&T2011, p.1496, plotted vs. daily average IMF B_Y values.

215

216

217 The similarity between the diagrams of Fig. 11 definitely constructed by post-event calculations (at

218 DTU Space) and those of Fig. 10 indicates beyond doubt that the latter have been derived by post-



219 event methods. From the post-event processing displayed in Figs. 10 and 11, the D- and H-
220 component solar wind sector terms appear highly correlated ($r = 0.95, 0.97$) with the daily mean
221 IMF B_Y values. Thus, they could be used to estimate past IMF B_Y levels and signs with good
222 probability from archived data. However, the objective according to the title and abstract of the
223 paper was to estimate IMF B_Y in near real time.

224 Compared to the D_{SS} and H_{SS} solar wind sector terms derived by post-event calculations displayed
225 in Figs. 10 and 11, the corresponding solar wind sector terms generated by using real-time
226 processing are much less well correlated with the daily average IMF B_Y values ($r = 0.67, 0.71$). The
227 relations displayed in Fig. 12 by the scattered D_{SS} and H_{SS} values derived by using near-real time
228 methods could hardly be used to determine the actual IMF B_Y magnitude level and sign with any
229 certainty, which was the main scope of the J&T2011 publication.

230

231

232 **Summary and conclusion**

233 The commented paper, J&T2011, and its replica in Troshichev and Janzhura (2012), are significant
234 since along with the publications Troshichev et al. (2006) and Troshichev et al. (2011) held in
235 chapter 4 of Troshichev and Janzhura (2012), they form the basis for the derivation procedures
236 (Matzka, 2014; Nielsen and Willer, 2019) applied for calculations of Polar Cap (PC) index values in
237 the near-real time and post-event (final) versions endorsed by IAGA Resolution #3 (2013).

238 However, neither the illustrations nor the results presented in J&T2011 have been derived by the
239 specified near-real time method. All the illustrations and results presented in Figs. 1, 6, 7, and 8
240 display values derived by post-event calculation methods based on daily median values smoothed
241 over 7 days centred on the day of interest. Figs. 2, 3, and 4 display observed values smoothed over 7
242 days, while the remaining Fig. 5 displays averages over 4 months.

243 In summary, there is strong disagreement between indications in the title, abstract, statements in the
244 text, and captions, as well as in the presentation of results, compared to re-calculations by rigorous
245 use of the presented near-real time procedure. Thus, it is concluded to caution against uncritical use
246 of the methods and results presented in the commented publication by Janzhura and Troshichev
247 (2011).

248

249

250 **Conflicts of interests.** The author declares that he has no conflict of interest with respect to the
251 present work.

252

253

254 **Data availability**

255 Geomagnetic data from Qaanaaq (THL) were supplied from the INTERMAGNET data service web
256 portal at <http://intermagnet.org>.

257 Solar wind plasma and magnetic field data based on data from the ACE, IMP, GeoTail, and WIND
258 space missions were supplied from the OMNIweb data service at <http://omniweb.gsfc.nasa.gov>.

259 Interim values of solar wind sector, H_{SS} and D_{SS} , and quiet day, QDC, values from PCN
260 calculations for 2001 were supplied by the index providers at DTU Space.

261

262



263 **Acknowledgments.** The staffs at the observatory in Qaanaaq its supporting institutes, the Danish
264 Meteorological Institute (DMI) and the Danish Space Research Institute (DTU Space), are
265 gratefully acknowledged for providing high-quality geomagnetic data for this study. The efficient
266 provision of geomagnetic data from the INTERMAGNET data service centre, the supply of solar
267 wind data from the IM8, WIND, GeoTail, and ACE missions, and the excellent performance of the
268 OMNIweb data portals are greatly appreciated. The author gratefully acknowledges the
269 collaboration and many rewarding discussions in the past with Drs. O. A. Troshichev and A. S.
270 Janzhura at the Arctic and Antarctic Research Institute in St. Petersburg, Russia.

271

272

273 **References:**

- 274 Janzhura, A. S., Troshichev, O. A.: Determination of the running quiet daily geomagnetic variation.
275 Journal of Atmospheric and Solar-Terrestrial Physics, 70, 962–972,
276 <https://doi.org/10.1016/j.jastp.2007.11.004> , 2008.
- 277 Janzhura, A. S., Troshichev, O. A.: Identification of the IMF sector structure in near-real time by
278 ground magnetic data, Ann. Geophys., 29, 1491-1500, [https://doi.org/10.5194/angeo-29-1491-](https://doi.org/10.5194/angeo-29-1491-2011)
279 [2011](https://doi.org/10.5194/angeo-29-1491-2011) , 2011.
- 280 Matzka, J.: PC_index_description_main_document_incl_Appendix_A.pdf, 2014. Available at DTU
281 Space web portal: <ftp://ftp.space.dtu.dk/WDC/indices/pcn/>
- 282 Nielsen, J. B. and Willer, A. N.: Restructuring and harmonizing the code used to calculate the
283 Definitive Polar Cap Index, Report from DTU Space, 2019. Available at:
284 <ftp://ftp.space.dtu.dk/WDC/indices/pcn/>
- 285 Stauning, P.: A critical note on the IAGA-endorsed Polar Cap index procedure: effects of solar
286 wind sector structure and reverse polar convection, Ann. Geophys., 33, 1443-1455,
287 <https://doi.org/10.5194/angeo-33-1443-2015> , 2015.
- 288 Stauning, P.: A critical note on the IAGA-endorsed Polar Cap (PC) indices: excessive excursions in
289 the real-time index values. Annales Geophysicae, 36, 621–631, [https://doi.org/10.5194/angeo-36-](https://doi.org/10.5194/angeo-36-621-2018)
290 [621-2018](https://doi.org/10.5194/angeo-36-621-2018) , 2018.
- 291 Troshichev, O. A. and Janzhura, A. S.: Space Weather monitoring by ground-based means, Springer
292 Praxis Books, Heidelberg, <https://doi.org/10.1007/978-3-642-16803-1> , 2012.
- 293 Troshichev, O. A., Janzhura, A. S., Stauning, P.: Unified PCN and PCS indices: method of
294 calculation, physical sense and dependence on the IMF azimuthal and northward components, J.
295 Geophys. Res., 111, A05208, <https://doi.org/10.1029/2005JA011402> , 2006.
- 296 Troshichev, O. A., Sormakov, D. A. : PC index as a proxy of the solar wind energy that entered into
297 the Magnetosphere: 3. Development of magnetic storms, J. Atmos. Solar-Terr. Phys.,
298 <https://doi.org/10.1016/j.jastp.2017.10.012> , 2017.

299